European Congress on Computational Methods in Applied Sciences and Engineering
ECCOMAS 2000
Barcelona, 11-14 September 2000

REGULARISED LIMIT ANALYSIS AND APPLICATIONS TO THE LOAD CARRYING CAPACITIES OF MECHANICAL COMPONENTS

F. Voldoire*

* Division Recherche & Développement (DRD)
Électricité de France
1, av. du Général de Gaulle, 92141 Clamart, France
e-mail: Francois.Voldoire@edf.fr, web page: http://www.edf.fr/html/en/index.html

Key words: Limit Analysis, numerical methods, structural analysis, elastoplasticity.

Abstract. *After a fast review of the methods proposed in the literature to calculate limit loads, we present the formulation of a regularisation method of the kinematical approach (upper bound method) of the limit analysis we have chosen, to obtain the collapse loads of any solid, obeying to the Von Mises strength criterion. It leads to mixed finite continuous elements. The advantage of this regularised formulation is to provide convergence theorems, leading to safe upper bounds associated to an estimated lower bound.*
This formulation has been implemented into the general purpose finite element software Code_Aster*, by introducing a specific constitutive relation and post-processing of the solution. Then, we give some numerical applications on 2D and 3D structures, making some comments on the advantages and drawbacks. We observed that in 2D plane strain situation, this algorithm is not very efficient without adaptive meshing, because the collapse mode present shear bands, hard to represent with continuous velocities fields. Nevertheless, the same method seems to be very efficient in 2D-axisymmetric and 3D situations.*

Finally, we have made a comparison with a direct analysis of an industrial component (2D-axisymmetric), using an elastoplastic finite strain simulation, to assess if another kind of failure mode (plastic snap-through) can occur. Indeed, the results are corroborated, and it appears that the efficiency of both simulations are quite similar.

1 INTRODUCTION

The aim of the limit analysis is the determination of the admissible loading of a mechanical structure, the geometry of which being fixed, constituted by materials satisfying a strength criterion, for instance a yield stress. We consider the case of combinations of any dead (constant) load and another parametrised by the loading factor, the maximum value of which we are seeking. The objectives of this study are to provide a F.E.M. tool to assess the safety of mechanical components with respect to the risk of plastic collapse, and to get some parameter needed in simplified fracture mechanics methods, like R6. Moreover, the limit analysis is an usefull tool for the geomechanical structures design.

After a review of the theoretical formulation and a brief summary of the proposed numerical methods in the literature, we present the kinematical regularised approach we have chosen, applied to von Mises yield criterion, by the Norton-Hoff-Frémond-Friaâ method, and implemented in the *Code_Aster*® software. We present the calculation of the numerical solutions of this non linear problem and the post-processing giving estimations of the limit loading factor. We summarise the results obtained during an european numerical benchmark (granted by a Brite EuRam project). Finally, we present the compared results of two idealisations of a particular pressurised component, with limit load and incremental finite elastoplastic analyses.

2 THEORETICAL FORMULATION OF THE LIMIT ANALYSIS

2.1 Definition of the limit load

We consider a body occupying the bounded domain Ω, submitted to surface loads $\lambda\mathbf{F}+\mathbf{F}_0$ on the boundary Γ_f, and body forces $\lambda\mathbf{f}+\mathbf{f}_0$ on Ω. A distinction is made between the loading $(\mathbf{F},\mathbf{f})$, parametrised by the positive scalar λ, and the dead or constant loading $(\mathbf{F}_0,\mathbf{f}_0)$. The homogeneous Dirichlet boundary conditions or perfect connections are applied on the complementary boundary Γ_u of $\partial\Omega$. Any non zero prescribed displacement nor anelastic initial strain - thermal, plastic… - have no effect on the admissible loading domain.

The constitutive material is characterised by a strength criterion, expressed by a scalar function of the stresses, negative for any admissible stress. For perfect-plastic material, with von Mises threshold, the criterion reads :

$$g(\sigma)=J(\sigma)-\sigma_y=\sqrt{3/2}.\sqrt{\sigma^D.\sigma^D}-\sigma_y=\frac{\sqrt{2}}{2}.\sqrt{(\sigma_1-\sigma_2)^2+(\sigma_2-\sigma_3)^2+(\sigma_1-\sigma_3)^2}-\sigma_y \qquad (1)$$

where :

- σ^D is the deviatoric stress tensor,
- σ_y is the strength for uniaxial tensile condition (as a yield stress), eventually depending on the localisation in the considered solid,
- σ_i being the principal stresses of the tensor σ.

This strength criterion being chosen, we are seeking to calculate the limit value of λ,

called the limit load factor or yield-point load $\lambda_{\lim}$, such as the solid can wear the loading $\lambda_{\lim}\mathbf{F}+\mathbf{F}_0$ and $\lambda_{\lim}\mathbf{f}+\mathbf{f}_0$.

Strictly speaking, the $\lambda_{\lim}$ value is the limit of the potentially supportable loading, but for materials satisfying the Maximal Plastic Work Principle, this value is the true value of the supported loading.

Two approaches are at our disposition for the yield design and limit analysis : the static approach (expressed in stress variables) and the kinematical approach (expressed in velocities variables). Both can be related to a mixed formulation, and lead, after numerical discretisation, to bounds of the limit load : a lower bound by the statical approach, an upper bound by the kinematical approach. When both values are the same, the obtained limit load is exact.

2.2 Mixed approach of the limit load

For the given load $(\mathbf{F},\mathbf{f})$, we define the kinematically admissible and normalised velocities space by :

$$\mathcal{V}_a^1 = \left\{ \mathbf{v} \text{ admissible, } \mathbf{v}=\mathbf{0} \text{ on } \Gamma_u \text{ , } \mathcal{L}(\mathbf{v}) = \int_\Omega \mathbf{f}.\mathbf{v}\, d\Omega + \int_{\Gamma_f} \mathbf{F}.\mathbf{v}\, ds = 1 \right\} \tag{2}$$

This normalisation corresponds to a unit work rate value of the load $(\mathbf{F},\mathbf{f})$. The dead load $(\mathbf{F}_0,\mathbf{f}_0)$ work rate is denoted by : $\mathcal{L}_0(\mathbf{v})$. From the strength criterion $\mathrm{g}(\sigma)$, we define :

a) the set of admissible stress tensors : $G_{(\mathbf{x})} = \left\{ \sigma(\mathbf{x}) \text{ , } \mathrm{g}(\sigma(\mathbf{x})) \le 0 \right\}$; ($G_{(\mathbf{x})}$ is convex, as well as g) ;

b) the indicatrix function : $\Psi_G(\sigma(\mathbf{x})) = \begin{cases} 0 \text{ , } si & \sigma(\mathbf{x}) \in G_{(\mathbf{x})} \\ +\infty \text{ , } si & \sigma(\mathbf{x}) \notin G_{(\mathbf{x})} \end{cases}$;

c) the support function : $\pi(\varepsilon) = \underset{\sigma \in \mathbb{R}^6}{\mathrm{Sup}} \left[\sigma.\varepsilon - \Psi_G(\sigma) \right]$.

We call Σ the space of the stress fields τ on Ω — whose regularity is such as we can define the internal work rate for any field from $\mathcal{V}_a$. For the sake of simplicity, we do not treat in the following the internal discontinuities surfaces of velocities, lying in the Ω body. Assume the lagrangian $S_m(\mathbf{v},\tau)$ ($\varepsilon(\mathbf{v})$ is the velocities strain tensor associated to $\mathbf{v}$), expressing the equilibrium equations and the belonging to the criterion G *via* the indicatrix function $\Psi_G(\tau)$, playing the role of a potential :

$$S_m(\mathbf{v},\tau) = \int_\Omega \left(\tau.\varepsilon(\mathbf{v}) - \Psi_G(\tau) \right) d\Omega - \mathcal{L}_0(\mathbf{v}) \tag{3}$$

The extreme load corresponds to the saddle-point of this lagrangian (because the maximisation in λ is included) :

$$\lambda_{\text{lim}} = \inf_{\mathbf{v}\in\mathcal{V}_a^1} \sup_{\tau\in\Sigma} \mathcal{S}_m(\mathbf{v},\tau) = \sup_{\tau\in\Sigma} \inf_{\mathbf{v}\in\mathcal{V}_a^1} \mathcal{S}_m(\mathbf{v},\tau) \tag{4}$$

2.3 Statical approach of the limit load (lower bound theorem)

The lower bound approach uses the stress fields defined in the space :

$$\Sigma_a^\lambda = \left\{ \tau \in \Sigma,\ \mathcal{W}(\mathbf{v},\tau) = \int_\Omega \tau.\varepsilon(\mathbf{v})\,d\Omega = \lambda \mathcal{L}(\mathbf{v}) = \lambda \quad ,\ \forall \mathbf{v} \in \mathcal{V}_a^1 \right\} \tag{5}$$

The extreme load factor is given by :

$$\lambda_{\text{lim}} = \sup_{\tau\in\Sigma_a^\lambda \cap G} \mathcal{S}_i(\tau), \text{ where : } \mathcal{S}_i(\tau) = \inf_{\mathbf{v}\in\mathcal{V}_a^1} \mathcal{S}_m(\mathbf{v},\tau) = \lambda - \int_\Omega \Psi_G(\tau^D)\,d\Omega \tag{6}$$

2.4 Kinematical approach of the limit load (upper bound theorem)

The Sup in the support function $\pi(\varepsilon)$ can be reached only if σ is chosen in $G_{(\mathbf{x})}$, such as : $\sigma = \lambda\varepsilon^D + \mu\mathbf{Id}$ (this ensures that $\sigma // \varepsilon^D$). The optimum corresponds to $g(\bar{\sigma}) = 0 \ \Rightarrow\ \bar{\lambda} = \sigma_y \sqrt{2/3}.\left(\varepsilon^D.\varepsilon^D\right)^{-1/2}$.

Then the support function reads : $\pi(\varepsilon(\mathbf{v})) = \sigma_y.\sqrt{\frac{2}{3}}\sqrt{\varepsilon(\mathbf{v}).\varepsilon(\mathbf{v})} + \sup_{\mu\in\mathbb{R}} \left(\mu.\text{div}\,\mathbf{v}\right)$. It is interpreted as the density of dissipable work rate through the $\varepsilon(\mathbf{v})$ at the material point. We can observe that the $\pi(\varepsilon)$ function is not differentiable at $\mathbf{0}$.

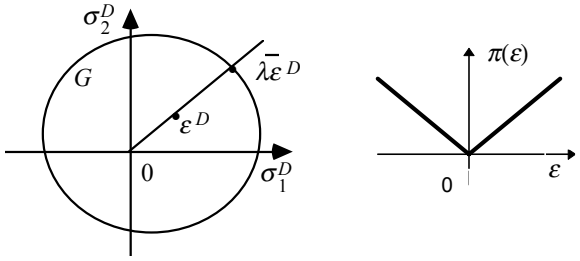

Figure 1: Optimum $\bar{\sigma}$ and graph of the support function $\pi(\varepsilon)$ in 1D situations.

The kinematical approach is defined by the convex functional $\mathcal{S}_e(\mathbf{v})$, which is positively homogeneous of degree one, for any $\mathbf{v} \in \mathcal{V}_a^1$, in the whole domain :

$$\mathcal{S}_e(\mathbf{v}) = \sup_{\tau\in\Sigma} \mathcal{S}_m(\mathbf{v},\tau) = \int_\Omega \pi(\varepsilon(\mathbf{v}))\,d\Omega - \mathcal{L}_0(\mathbf{v}) \tag{7}$$

This functional is the integral on the body of the support function π of the convex $G_{(\mathbf{x})}$, calculated for the $\varepsilon(\mathbf{v})$ strain rate, and can be interpreted as the maximal dissipable work rate in the velocities field $\mathbf{v}$ (the contribution of the interface strength vanishing). The support function π being positively homogeneous of degree one, consequently the functional $\mathcal{S}_e(\mathbf{v})$ is too. With the von Mises criterion, the dissipable work rate functional $\mathcal{S}_e(\mathbf{v})$ reads :

$$\mathcal{S}_e(\mathbf{v}) = \int_\Omega \left[\sigma_y . \sqrt{\frac{2}{3}} \sqrt{\varepsilon(\mathbf{v}).\varepsilon(\mathbf{v})} + \operatorname*{Sup}_{q \in \mathbb{R}} \left(q.\operatorname{div} \mathbf{v} \right) \right] d\Omega - \mathcal{L}_0(\mathbf{v}) \tag{8}$$

We can observe that only the $\mathbf{v}$ fields belonging to the subspace $C = \left\{ \mathbf{v} \in \mathcal{V}_a^1 \text{ , } \operatorname{div} \mathbf{v} = 0 \text{ dans } \Omega \right\}$ give finite values of $\mathcal{S}_e(\mathbf{v})$. The $\mathbf{v}$ fields have to satisfy the isochoric condition : $\operatorname{div} \mathbf{v} = \operatorname{tr} \boldsymbol{\varepsilon}(\mathbf{v}) = 0$. It is why we need incompressible finite elements to perform the calculation of limit load factor with the von Mises criterion. The (quite general) method used to deal with the incompressibility may consist in mixed finite elements (velocities, mean pressure), ensuring by dualisation the isochoric condition in a weak form. These elements have to verify the so-called LBB condition, to avoid spurious solutions. The limit load factor λ_{lim} given by the kinematical approach is the solution of this optimisation problem :

$$\lambda_{\text{lim}} = \operatorname*{Inf}_{\mathbf{v} \in \mathcal{V}_a^1} \mathcal{S}_e(\mathbf{v}) = \operatorname*{Inf}_{\substack{\mathbf{v} \in \mathcal{V}_a \\ \mathcal{L}(\mathbf{v}) > 0}} \frac{\mathcal{S}_e(\mathbf{v})}{\mathcal{L}(\mathbf{v})} = \operatorname*{Sup}_{\lambda > 0} \operatorname*{Inf}_{\mathbf{v} \in \mathcal{V}_a^1} \left(\mathcal{S}_e(\mathbf{v}) - \lambda \left(\mathcal{L}(\mathbf{v}) - 1 \right) \right) \tag{9}$$

When the optimum is reached, we get a solution $\mathbf{u}$ and the limit load factor λ_{lim} ; there is no uniqueness of the field $\mathbf{u}$, but λ_{lim} is unique. Any loading combination $\mathcal{L}_0(\mathbf{v}) + \lambda \mathcal{L}(\mathbf{v})$ with $0 \le \lambda \le \lambda_{\text{lim}}$ is supportable. Beyond λ_{lim}, the equilibrium problem violates the strength criterion.

3 REVIEW OF NUMERICAL TECHNIQUES IN THE LIMIT ANALYSIS

Implementation the numerical of the lower and upper bounds methods presented above leads to difficulties. The first one requires the construction of statically admissible stress fields, which is delicate (excepted certain 2D cases), on which one must check the not exceeding of the criterion. The second one frequently provides interesting results only to the condition of choosing of discontinuous velocities fields, which are difficult to introduce into the finite elements. It however requires the minimisation of a not-differentiable functional (close to that of the problems of elastoplastic damage mechanics).

One finds very few « industrial » versions of computational softwares dealing with limit analysis. This is due primarily to the low number of applications under consideration compared to the practice in calculation of the structures (in elasticity or elastoplasticity for example). However, the general balance-sheet of the methods tested by various authors makes

it possible the choice of algorithms. Those presented in the literature can be classified according to three following groups :

~~Lower bound method~~	~~Upper bound method~~	~~Mixed method~~
1. Criterion and nonlinear programming on discontinuous stresses 2. Criterion and nonlinear programming with a basis-reduction technique of the stress space 3. Linearisation of the criterion and linear programming 4. Criterion and iterative weak admissible elastic-rigid stress fields by FEM.	1. Heuristic minimisation with discontinuous velocities 2. Linearisation of the criterion and linear programming with discontinuous velocities 3. Partition and partial regularisation with discontinuous velocities 4. Norton-Hoff regularisation, with continuous velocities.	1. Linearisation of the criterion and linear programming, with continuous velocities and discontinuous stresses 2. Bingham regularisation by projection with continuous velocities and collocation for the stresses 3. Norton-Hoff regularisation, continuous stresses and velocities.

Table 1 : Main algorithms characteristics.

3.1 Lower bound numerical methods of the limit load

The principal characteristics of the lower bound method are : the construction of statically admissible stress fields ; the resolution of the problem of optimisation with checking of the criterion everywhere. Historically, Hodge and Belytschko [i] were among the first to treat the 2D plane cases and plates. The selected discretisation also consists of finite elements with stresses d.o.f. (derived from an Airy's function). The conditions of connection on the elements edges are exploited to eliminate from the d.o.f. Discontinuities can be considered only between two elements. A nonlinear programming algorithm of minimisation is used.

Casciaro [ii] *et al*. underline the cost of the checking of the criterion on each element, caused by the choice of a quadratic discretisation of the stress. They propose on the contrary a linear discretisation, which makes it possible to limit the checking of the criterion on the nodes of the mesh. A linearisation of the criterion per pieces makes it possible to use algorithms employed in linear programming, which are very effective. For the Von Mises case, one would need 32 linear inequations to approach it with less than 5%. Christiansen [iii] did this choice too to avoid very expensive problem of optimisation.

This strategy was also used by Pastor [iv] *et al* in a case adapted to the axisymmetric problems. They used P1 stress finite elements, where 2 linear relations of continuity between the common edges are taken into account. In the Coulomb's case, the criterion is linearised per pieces, the cone being replaced by a polyhedron. Of course, the found limit loads will be only upper limits for the real problem with the criterion of non associated Coulomb. Once linearised, the criterion is calculated at the nodes, where the extrema are reached.

More recently, Heitzer [v] has proposed to use a basis-reduction technique of the residual stress space (the elastic solution being chosen to equilibrate the external loading) so thet the cost of the nonlinear programming becomes not excessive.

Another way was proposed by Ponter : the use of elastic finite elements to build by an iterative procedure a sequence of equilibrated stress fields (in a weak sense), by a progressive smoothing of zones where the criterion is reached.

3.2 Mixed approach numerical methods of the limit load

This method introduce multipliers, according to the Kühn-Tucker's theorem. The potential risk lies in a bad conditionning : some people prefer to devote to the direct problem. The mixed methods (leading to a saddle-point problem) have the advantage of revealing at the same time the stress field and the velocities field in the collapse, and producing directly a bounding of the limit load factor.

Casciaro *et al.* proposed an association of linear elements for velocities as for the stresses, with discontinuities between elements, and with an *a priori* incompressibility of the velocities fields, or imposed with a dual form. Discretisation of Lagrangian resulted in checking the balance and the law of flow to the weak direction only; on the other hand, it is required that the criterion be never violated, nor kinematic admissibility. Christiansen proposed a little different method, with constant stress elements. A convergence theorem was established.

Other works proposed not to linearise the criterion, like Zouain *et al*. [vi], but a Newton-like algorithm, replacing the hessian by a positive definite matrix, directly on the conditions of optimality of the lagrangian.

3.3 Upper bound numerical methods of the limit load

Due to the difficulty lying in the not-differentiable character of the potential defining the strength criterion of material, many authors proposed either a method of regularisation, to replace this potential (or its dualised form) by another which is differentiable, « adjustable » by a parameter, of which the limiting value led to convergence towards the preceding potential, or a heuristic minimisation, without the need of the hessian.

The method of heuristic minimisation of the function $S_e(\mathbf{v}_h)$, (used for instance by Maghous [vii], with constant or linear continuous fields $\mathbf{v}_h$) although very simple to implement and general, seems expensive and sensitive to the choice of the starting point. Its users associate it with a partitioning according to zones of the structure non concerned by the collapse flow (given roughly by some iterations of nonlinear programming).

The linearisation of the criterion makes it possible to use the fast methods of linear optimisation, but it can provide however results further away from the exact extreme loads (see for instance Casciaro, Pastor [viii] with P1 elements…).

The incompressibility is sometimes treated in a way approached by penalisation, while adding to Lagrangian term in $(\operatorname{div}\mathbf{v})^2$, affected of a great coefficient. If not, it is treated by Lagrange's multipliers and an Uzawa's algorithm on the dual problem.

A first regularisation of the $S_e(\mathbf{v}_h)$ functional, basic approach if one can say, consists in adding in the expression of the function of support of convex constant term making it derivable at 0, see for instance Clément [ix], Gaudrat [x] … Of course, the problem of

minimisation of the functional ${}^{\alpha}S_e(\mathbf{v})$ thus obtained is very badly conditioned when α tends towards 0 (the gradient and the hessian are difficult to calculate numerically).

One can classify the method suggested by Yan [xi] in this category : he used a regularisation by a fictitious perfectly plastic viscous flow potential, where the Young's modulus plays the role of parameter ; the incompressibility is treated in the same manner, by penalisation.

Another approach uses laws of viscous behaviour, where the parameter of regularisation is interpreted like a viscosity. A method by projection on the criterion $G_{(\mathbf{x})}$ was proposed by Mercier [xii]. He chose a law of the Bingham-Perzyna type, where the flow takes place only with the crossing of the threshold; the potential which replaces the indicatrix function $\Psi_G(\sigma)$ of convex having the form : $\Psi_G^{BP}(\tau(\mathbf{x})) = \frac{1}{2\mu}\left\|\tau(\mathbf{x}) - \Pi_G(\tau(\mathbf{x}))\right\|^2$.

The Mercier's regularised functional derived from $S_e(\mathbf{v})$ reads :

$$ {}^{\mu}S_e(\mathbf{v}) \;=\; S_e(\mathbf{v}) + \int_\Omega \frac{\mu}{2}\|\varepsilon(\mathbf{v})\|^2 d\Omega \tag{10}$$

Instead of regularising the functional to be optimised, one finds also algorithms which exploit the presence of the rigid zones in the optimal solutions by a « partition », while being reduced to the optimisation of a differentiable functional. Unfortunately, these algorithms do not cross to a stage of regularisation, to deal with the complete problem. One can wonder, if the use of a method of adaptive meshing, coupled with the methods seen higher, could not be even more effective.

Finally, it seems interesting to use the method of regularisation by the Norton-Hoff's viscous law (with a coefficient of « viscosity » $\mu > 0$), both on the upper bound method or on the mixed approach. Historically, it seems that it is in the precursory work of Casciaro in 1971, that one finds a first application of this regularisation. Associated with a mixed method, it led to a computational software « LIMAN », see the Casciaro's paper. In 1982, these authors proposed this regularisation to the mixed approach. This regularisation was studied in detail by Friaâ [xiii] in 1979. The indicatrix function $\Psi_G(\tau)$ is regularised in the following way, $q > 1$ (expressed with the gauge function $j(\tau)$ of the convex $G_{(\mathbf{x})}$) :

$$\Psi_G^{NH}(\tau(\mathbf{x})) = \frac{\mu}{q}\left(j(\tau(\mathbf{x}))\right)^q \tag{11}$$

Casciaro proposed also to choose the following expression of the regularised potential :

$$\Psi_G^{NHq}(\tau) \;=\; \left(\frac{1}{|\Omega|}\int_\Omega \left(\mathrm{g}(\tau) + \sigma_y\right)^q \sigma_y^{-q}\, d\Omega\right)^{1/q} \tag{12}$$

Figure 2 allows to compare in the one-dimensional case (the convex is represented by the segment $]-\sigma_y,\ \sigma_y[$) these potentials with the original non differentiable potential.

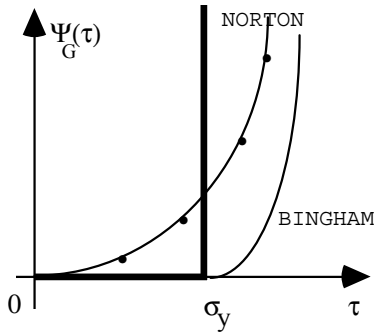

Figure 2: Comparison of regularised potentials in 1D case.

The form of the coercive Norton-Hoff potential leads to place itself in functional spaces in duality of the type L^p, $p>1$, and L^q where the sum $p^{-1}+q^{-1}=1$. We get good properties on the solutions : they become regular, and for $p=q=2$ that leads to a problem of linear viscosity. And the solution of the initial collapse problem corresponds to the limit of the normalised sequel of the solutions $\left(\mathbf{u}_q,\sigma_q\right)$, for $q\to\infty$; by post-processing, we get decreasing values of the limit load factor. Its initialisation rests on a linear calculation. A same technique was used for instance by Guennouni [xiv] or recently by Berak [xv].

3.4 Choice of a numerical method of the limit load

One can summarise the advantages and the disadvantages of the various methods suggested in the literature as follows. The lower bound methods, in their « exact » version are limited to the 2D or plate-bending cases, and their cost is noticeable. It seems that linearising the criterion leads to poor results. In their « weak » (in the sense of verifying the equilibrium equations) version, with reduction technique, they appear efficient, but needs a special implementation in usual finite element codes. For the treatment of the upper bound method, it appears that the regularisation is a good way, with a special mention to the Norton-Hoff one, because of its convergence properties. That is why we have decided to implement the upper bound approach, with the Norton-Hoff-Frémond-Friâa method into a general purpose non linear mechanical software uses displacement formulated finite elements, namely *Code_Aster* : we only need to implement the Norton-Hoff constitutive relation.

4 NORTON-HOFF REGULARISATION OF THE UPPER BOUND METHOD

4.1 Theoretical formulation

We regularise the non-differentiable functional $\mathcal{S}_e(\mathbf{v})$ by the Norton-Hoff method. We replace the support function $\pi(\varepsilon)$ by the regularised and differentiable support function $\pi^{NH}(\varepsilon)$. It is adjustable by a regularisation parameter n $(1\le n\le+\infty)$, which limit value $n\to+\infty$ gives the convergence to support function $\pi(\varepsilon)$:

$$\pi^{NH}(\varepsilon) \;=\; \frac{nk^{-1/n}}{1+n}\left(\pi(\varepsilon)\right)^{\frac{1+n}{n}} \tag{13}$$

In the *Code_Aster*, we chose the constant $k=\sigma_y^2/3\mu$, in order to recover the elastic incompressible problem, when $n=1$ (2μ being the second Lamé's coefficient).

We denote the space of the admissible velocities, adapted to the viscous flow, through the Norton-Hoff constitutive relation of order n :

$$\mathcal{V}_a^{n\,1}=\left\{\,\mathbf{v}\in L^n(\Omega)\,,\quad and\quad \varepsilon(\mathbf{v})\in L^n(\Omega)\,,\quad \mathbf{v}=0\ on\ \Gamma_u\,,\quad \mathcal{L}(\mathbf{v})=1\,\right\} \tag{14}$$

We define on this space the regularised functional $S_e^n(\mathbf{v})$:

$$S_e^n(\mathbf{v})=\int_\Omega \frac{nk^{-1/n}}{n+1}\pi\left(\varepsilon(\mathbf{v})\right)^{\frac{1+n}{n}}\,d\Omega-\mathcal{L}_0(\mathbf{v}) \tag{15}$$

The minimisation problem $\underset{\mathbf{v}\in\mathcal{V}_a^{n\,1}}{\mathrm{Inf}}\left[S_e^n(\mathbf{v})\right]$ is well-posed thanks to the properties of the spaces $L^n(\Omega)$ (due to the Hölder inequality) and has a unique solution $\mathbf{u}_n$, for which the reached value of the Inf is : λ_n. We show that this problem can also be written as the seeking of the saddle-point $\left(\lambda_n,\mathbf{u}_n,p_n\right)$ of the following lagrangian :

$$\underset{\lambda\in\mathbb{R}}{\mathrm{Max}}\ \underset{\mathbf{v}\in\mathcal{V}_a}{\mathrm{Inf}}\ \underset{q\in \mathrm{L}^2(\Omega)}{\mathrm{Sup}}\int_\Omega A(n).\left(\sqrt{\varepsilon(\mathbf{v}).\varepsilon(\mathbf{v})}\right)^{\frac{1+n}{n}}\,d\Omega+\int_\Omega q.\mathrm{div}\,\mathbf{v}\,d\Omega-\mathcal{L}_0(\mathbf{v})-\lambda\left(\mathcal{L}(\mathbf{v})-1\right) \tag{16}$$

with : $A(n)=\dfrac{n}{1+n}\sigma_y{}^{(n-1)/n}\left(3\mu\right)^{1/m}\left(\dfrac{2}{3}\right)^{\frac{1+n}{2n}}$. In practice, we take the sequence : n = 1, 10, …, ∞, and $A(n)$ is decreasing (if $E\geq\sigma_y$) from 2μ to $\sigma_y\sqrt{\dfrac{2}{3}}$ keeping homogeneous to a stress, and remaining bounded.

This lagrangian eq. [16] allows to force directly in the operator the isochoric condition as well the normalisation to 1 of the work rate of loading. Then we build a decreasing sequence of λ_n values and the limit load factor λ_{lim} is the limit of this sequence when $n\to+\infty$:

$$\lambda_{\mathrm{lim}} \;=\; \lim_{n\to+\infty}\left(\underset{\mathbf{v}\in\mathcal{V}_a^{n\,1}}{\mathrm{Inf}}\left[S_e^n(\mathbf{v})\right]\right)=\lim_{n\to+\infty}\left(S_e^n\left(\mathbf{u}_n\right)\right) \tag{17}$$

We can refer to Friaâ and Frémond to see the proof. We show also the following property of the solutions of eq.[9]. If we amplify the loading $\mathcal{L}\to\beta\mathcal{L}$, when $\mathcal{L}_0=0$, the solutions depend on β by the following relationships :

$$\mathbf{u}_n(\beta)=\beta^{-1}\mathbf{u}_n(1)\ ; \qquad p_n(\beta)=\beta^{-1/n}p_n(1) \tag{18}$$
$$\sigma^D(\mathbf{u}_n(\beta))=\beta^{-1/n}\sigma^D(\mathbf{u}_n(1)); \quad \mathcal{S}_e^n(\mathbf{u}_n(\beta))=\beta^{-(1+n)/n}\mathcal{S}_e^n(\mathbf{u}_n(1))$$

One of the advantages of this regularising method lies in the embedding property of the spaces $L^n(\Omega)$, that leads to an interesting property of the λ_n sequence, see paragraph 4.4. So we get the proof of the following properties, for a bounded body Ω, denoting $|\Omega|=\int_\Omega d\Omega$ and $\|\Omega\|_n=\int_\Omega A(n)d\Omega$: For any $1\le n$ and $1\le r\le s$ and any field $\mathbf{u}$ in $\mathcal{V}_a^n$, we have :

$$\int_\Omega A(n)\sqrt{\varepsilon(\mathbf{u}).\ \varepsilon(\mathbf{u})}d\Omega\le\|\Omega\|_n^{\frac{r-1}{r}}\left(\int_\Omega A(n)(\varepsilon(\mathbf{u}).\ \varepsilon(\mathbf{u}))^{\frac{r}{2}}\ d\Omega\right)^{\frac{1}{r}}\le\|\Omega\|_n^{\frac{s-1}{s}}\left(\int_\Omega A(n)(\varepsilon(\mathbf{u}).\ \varepsilon(\mathbf{u}))^{\frac{s}{2}}\ d\Omega\right. \tag{19}$$

$$\int_\Omega\sigma_y.\sqrt{\tfrac{2}{3}\varepsilon(\mathbf{u}).\varepsilon(\mathbf{u})}\,d\Omega\le|\Omega|^{1/(n+1)}\left(\int_\Omega\sigma_y{}^{(n+1)/n}.\left(\sqrt{\tfrac{2}{3}\varepsilon(\mathbf{u}).\varepsilon(\mathbf{u})}\right)^{(n+1)/n}d\Omega\right)^{n/(n+1)}\qquad\forall\mathbf{u} \tag{20}$$

These properties are interesting because they remain true for heterogeneous materials, and we can consider the yield stress either as measure (as a specific mass) or as belonging to the strain energy.

4.2 Numerical aspects of the limit load calculation with *Code_Aster*

The weak form of the optimisation problem reads as following :

The coefficient n given, find $(\lambda_n,\mathbf{u}_n,p_n)\in\mathbb{R}\times\mathcal{V}_a\times\mathrm{L}^2(\Omega)$ such as :

$$\begin{cases}\int_\Omega A(n).\left(\sqrt{\varepsilon(\mathbf{u}_n).\ \varepsilon(\mathbf{u}_n)}\right)^{(1-n)/n}\ \varepsilon(\mathbf{u}_n).\ \varepsilon(\mathbf{v})d\Omega+\int_\Omega p_n.\mathrm{div}\mathbf{v}\,d\Omega-\lambda_n\mathcal{L}(\mathbf{v})=\mathcal{L}_0(\mathbf{v})\ \forall\mathbf{v}\ \in\mathcal{V}_a\\ \int_\Omega q.\mathrm{div}\mathbf{u}_n\,d\Omega\ =0\ \ \forall q\ \in\mathrm{L}^2(\Omega)\\ \mathcal{L}(\mathbf{u}_n)\ =1\end{cases} \tag{21}$$

This problem admits an unique solution for any $n\ge1$. For n=1 the problem is of linear incompressible elasticity type. We get an estimation of the limit load factor by an upper bound, the $\mathbf{u}_n$ field giving an idea of a collapse mode. For the incompressibility treatment, we refer to the weak mixed formulation :

$\int_\Omega q.\mathrm{div}\mathbf{u}d\Omega\ +\int_\Omega\frac{q.p}{\xi}d\Omega=0,\forall q\in\mathrm{L}^2(\Omega)$, the penalisation term $\int_\Omega\frac{q.p}{\xi}d\Omega$ avoiding some difficulties with a LDLT-like linear algebra solver and corresponding to a Poisson's ratio like ν=0.4999... ($\xi\to\infty$ when $\nu\to0.5$). Then the solutions are only quasi-incompressible.

The variational formulation eq. [21] is solved by the popular non linear iterative Newton-Raphson algorithm by *Code_Aster* (including other ingredients like line-search, continuation…), with mixed 2D and 3D finite elements (Taylor-Hood), defined by the

degrees of freedom vector $(\mathbf{U},\mathbf{P})$, on the spaces $\mathcal{V}_0$ and Q of discretised functions.

The stress tensor $\sigma(\mathbf{u})$ satisfies the Norton-Hoff constitutive relation, integrated by an implicit method. The deviatoric stress associated to the strain rate is :

$$\sigma^D(\mathbf{u}) = \frac{1+n}{n} A(n) \left(\sqrt{\varepsilon^D(\mathbf{u}).\varepsilon^D(\mathbf{u})} \right)^{(1-n)/n} .\varepsilon^D(\mathbf{u}) \tag{22}$$

We need the tangent operator $\left.\frac{d\sigma}{d\varepsilon}\right|_{\varepsilon(\mathbf{u})}$, applied to any deviatoric tensor $\mathbf{e}$:

$$\frac{d\sigma^D}{d\varepsilon^D}.\mathbf{e} = A(r) \left(\sqrt{\varepsilon^D(\mathbf{u}).\varepsilon^D(\mathbf{u})} \right)^{(1-r)/r} \left(\mathbf{e} + \left(\frac{1-r}{r} \right) \frac{\varepsilon^D(\mathbf{u}) \otimes \varepsilon^D(\mathbf{u})}{\varepsilon^D(\mathbf{u}).\varepsilon^D(\mathbf{u})} .\mathbf{e} \right) \tag{23}$$

The second member $\int_\Omega \sigma(\mathbf{u} + \Delta\mathbf{u}_i).\varepsilon(\mathbf{v}) d\Omega$ is updated, through the computing of the stress field from the constitutive relation. The tangent operator $\left.\frac{d\sigma}{d\varepsilon}\right|_{\varepsilon(\mathbf{u}+\Delta\mathbf{u}_i)}$ is also updated on request, at certain iteration i only, to avoid an expensive assembling of the stifness matrix.

In our case, the solving can be achieved without time-discretisation, but it is interesting to update the tangent stiffness time to time to speed-up the convergence. We use a LDLT type solver ; the normalisation equation, coupling a lot of degree of freedom being reported at the bottom of the equations system. We can prefer to make a break in the calculation, or restart from any previous solution $(\mathbf{u}, p)$, even obtained from another parameter n : this enables computing time reduction. In any case, it is recommended to begin a calculation with a coarse mesh to evaluate the effect of the parameter n on the λ_n values.

4.3 Post-processing and calculation of the limit load factor

The solution $(\lambda_n, \mathbf{u}_n, p_n)$ being calculated, for a given n, we have to use the λ_n sequence to build the approximation of the limit load factor. We make profit of the properties eq. [19], the fact that $A(n)$ is decreasing, and the property coming from the minimisation eq. [17]. For $1 \le r \le s$, we conclude that for $\mathbf{u}_r$ and $\mathbf{u}_s$ respectively solutions (satisfying also the incompressibility and normalisation conditions) of eq. [17] for $n = r$ and $n = s$:

$$\int_\Omega A(r) \sqrt{\varepsilon(\mathbf{u}_r).\ \varepsilon(\mathbf{u}_r)} d\Omega \le \|\Omega\|_r^{\frac{r-1}{r}} \left(\int_\Omega A(r) (\varepsilon(\mathbf{u}_r).\ \varepsilon(\mathbf{u}_r))^{\frac{r}{2}}\ d\Omega \right)^{\frac{1}{r}} \le \|\Omega\|_s^{\frac{s-1}{s}} \left(\int_\Omega A(s) (\varepsilon(\mathbf{u}_s).\ \varepsilon(\mathbf{u}_s))^{\frac{s}{2}}\ d\Omega \right. \tag{24}$$

We denote by $\widetilde{\lambda}_n$ the terms of the sequence (decreasing for $n \to +\infty$ and converging to λ_{lim}), that we calculate in practice by post-processing from $\mathbf{u}_n$ (the loading work rate being equal to 1) :

$$\widetilde{\lambda}_n = \|\Omega\|_n^{1/(1+n)} \left(\int_\Omega A(n) (\varepsilon(\mathbf{u}_n).\varepsilon(\mathbf{u}_n))^{\frac{1+n}{2n}}\ d\Omega \right)^{n/(1+n)} - \mathcal{L}_0(\mathbf{u}_n) \tag{25}$$

As we can make a minoration (knowing that $A(+\infty)=\sigma_y\sqrt{\frac{2}{3}}$) of the first term of eq. [20] we calculate then the decreasing sequence $\hat{\lambda}_n$ for $n\to+\infty$ converging also to λ_{lim} :

$$\lambda_{lim}\le\hat{\lambda}_n=\int_\Omega\sigma_y\sqrt{\tfrac{2}{3}\varepsilon(\mathbf{u}_n).\varepsilon(\mathbf{u}_n)}\;\;d\Omega\;-\mathcal{L}_0(\mathbf{u}_n)\le\widetilde{\lambda}_n \tag{26}$$

The precision of the approximation of the limit load factor λ_{lim} is determined by comparison of the different values of $\hat{\lambda}_n$ that converge to λ_{lim} from above (at $n\to+\infty$). These terms are calculated by numerical integration at the Gaussian points of the finite elements. Another interpretation of the interest of making profit of this sequence lies in the fact that it uses directly the expression of the support function of the strength convex, that is the dissipable work rate in the potential collapse modes, applied to the incompressible and normalised solutions $\mathbf{u}_n$.

If the dead loading vanishes : $\mathcal{L}_0=0$, we can post-process the stress field (quasi statically admissible) coming from the solution $\mathbf{u}_n$ and get an estimated value of the limit load factor, which would be a lower bound if the equilibrium equations were exactly fulfilled. We calculate then the sequence $\underline{\lambda}_n$, which has not - unfortunately - any property of monotony :

$$\underline{\lambda}_n=\int_\Omega A(n).\left(\sqrt{\varepsilon(\mathbf{u}_n).\varepsilon(\mathbf{u}_n)}\right)^{(1+n)/n}d\Omega.\left(\operatorname*{Sup}_{\mathbf{x}\in\Omega}\left(\frac{\sqrt{\frac{3}{2}\boldsymbol{\sigma}^D(\mathbf{u}_n).\boldsymbol{\sigma}^D(\mathbf{u}_n)}}{\sigma_y}\right)\right)^{-1}\le\hat{\lambda}_n \tag{27}$$

This maximisation (of the gauge function of the strength convex) is calculated only at the Gaussian points of the finite elements. So the obtained value, for each n, lower than $\hat{\lambda}_n$, can only be considered as an indication.

5 VALIDATION TEST

5.1 Reference problem

We consider a rectangular plate or a hexahedron or an axisymmetrical cylinder (inner radius 1mm, outer radius 2mm). The homogeneous material satisfies the von Mises strength criterion (with the threshold σ_y). The body is subjected to pressures on the horizontal boundary $-\alpha f$ and on the vertical (inner) boundary $-(1-\alpha)f$ with $\alpha\ge 0.5$. With this very simple sample problem, an analytical calculation enables to get the exact limit load factor, as well the estimations by the regularisation method.

5.2 Plane case

The solid is submitted to pressures on the horizontal boundary : $-\alpha f$ and vertical one : $-(1-\alpha)f$, with : $\alpha\ge 1/2$, and the z-displacement is zero. We consider two ways to control the loading : in the case1 : both pressures (horizontal and vertical) are parametrised by λ, in

the case2 : the horizontal pressure is parametrised by λ, while the vertical pressure remains constant $-(1-\alpha)f_0$, with $f_0 = \lambda_0 f$. The plane strain solution is homogeneous. We get the limit load factor for these loading directions, for von Mises criterion, with the threshold σ_y :

case	Limit analysis solution load factors	Regularised limit analysis solution sequence terms of load factors
1	$\lambda_{\lim}.f = \dfrac{2\sqrt{3}\sigma_y}{3.\lvert 2\alpha-1\rvert}$	$\hat{\lambda}_n.f = \dfrac{2\sqrt{3}\sigma_y}{3.\lvert 2\alpha-1\rvert}$, $\forall n$; $\underline{\lambda}_n.f = \dfrac{2n\sqrt{3}\sigma_y}{3(1+n).\lvert 2\alpha-1\rvert}$
2	$\lambda_{\lim}.f = \dfrac{2\sqrt{3}\sigma_y}{3.\lvert\alpha\rvert} + \dfrac{1-\alpha}{\lvert\alpha\rvert}\lambda_0.f$	$\hat{\lambda}_n.f = \dfrac{2\sqrt{3}\sigma_y}{3.\lvert\alpha\rvert} + \dfrac{1-\alpha}{\lvert\alpha\rvert}\lambda_0.f \quad \forall n$

Table 2 : Plane case : direct and regularised limit analysis.

The invariance in n which can be observed here comes from the fact that the equilibrated stress field is unique. For the case1, we get the exact limit load factor $\lambda_{\lim}$ when $n \to +\infty$.

5.2 Axisymmetrical case

For the 2D axisymmetrical case, we consider the same geometry, but the solid, the axial displacement of which vanishing, is submitted to the only pressure on the inner wall : αf parametrised by λ. The stress field is not homogeneous.

Limit analysis load factor	Regularised limit analysis solution sequence terms of load factors
$\lambda_{\lim}.\alpha f = \dfrac{2\sqrt{3}}{3}\sigma_y \ln\dfrac{b}{a}$	$\hat{\lambda}_n.\alpha f = \dfrac{2\sqrt{3}}{3}\sigma_y \ln\dfrac{b}{a}$, $\forall n$; $\underline{\lambda}_n.\alpha f = \dfrac{n^2\sigma_y\sqrt{3}}{3(1+n)}\dfrac{b^{-1/n}-a^{-1/n}}{a^{-1/n}}$

Table 3 : Axisymmetrical-case : direct and regularised limit analysis results.

For $n \to +\infty$, we get the convergence : $\underline{\lambda}_{+\infty} = \underline{\lambda}_{\lim}$.

5.3 Three-dimensional case

In 3D we consider the same geometry, but the solid, of unit thickness, is free in the antiplane z direction. The solid is submitted to pressures applied on the horizontal boundary : $-\alpha f$ and vertical one : $-(1-\alpha)f$, with : $\alpha \geq 1/2$. Both pressures are parametrised by λ.

Limit analysis load factor	Regularised limit analysis solution sequence terms of load factors
$\lambda_{\lim}.f = \dfrac{\sigma_y}{\sqrt{3\alpha^2-3\alpha+1}}$	$\hat{\lambda}_n.f = \dfrac{\sigma_y}{\sqrt{3\alpha^2-3\alpha+1}}$

Table 4 : Three-dimensional case : direct and regularised limit analysis results.

6 BENCHMARK ON VARIOUS TYPICAL PROBLEMS

Some European partners have shared the specifications (and the F.E. meshes) of tests of limit analysis. These benchmarking tests (partly funded by a Brite-EuRam project BE97-4547) concern : a plate under tension with a centred hole, a heterogeneous plate under tension with a crack (LA3) , an axisymmetric cracked tube under pressure and tension (LA4), a pressurised tube with a three-dimensional defect (LA5), a vessel-head under pressure (LA6). We achieved the numerical calculations with the *Code_Aster*® of the tests LA3, LA4, LA5, LA6. In this section, we present the main results.

LA3 : Plate with a centered crack under tension

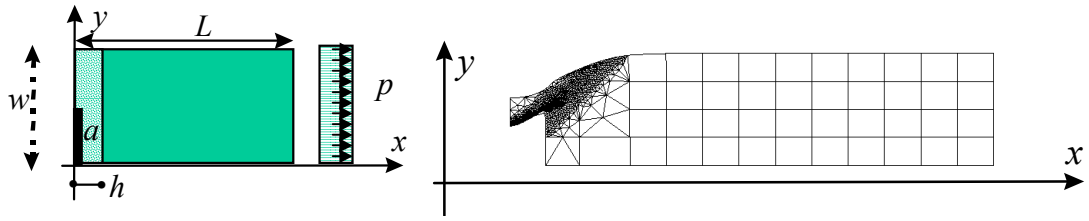

Figure 3: Tensile plate with a centered crack ; deformed mesh (right) with 2D plane strain Q8, T6 elements .

material	heterogeneous (base and weld metals)
constitutive relation	perfect plasticity ; $\sigma_y{}^B = 100\,MPa$; $\sigma_y{}^W / \sigma_y{}^B$: 0.5->1.5.
geometry	crack : a/w=0.5 ; h/w=0.3 ; L=4.w=4mm.

Table 5 : Plate with a centered crack : data.

Our results by limit analysis regularisation algorithm implemented into the *Code_Aster* are presented in the table 6 (the analytical values come from Joch *et al.* [xvi]). The number of equivalent elastic computations (to get an idea of the computing cost) is between 52 and 100, while the regularisation parameter n remains limited to 15,5. In this case, we are in the presence of a discontinuous solution that the algorithm tries to approach with continuous solutions, which explains the appearance in the deformation of a transitory zone between the two blocks, which is a zone allowing to pass continuously from one block to the other. That explains why the sequence of solutions has difficulties to converge. It appears that adaptive meshing coupled with this algorithm will be a necessary tool in 2D situations, in order to catch the shear band. Other continuous upper bound methods have the same difficulties.

$\sigma_y{}^W / \sigma_y{}^B$	0,50	0,75	1,00	1,25	1,50
$F_{\lim}^{anal}$ (N.mm^{-1})	64,66	95,84	115,47	131,64	146,65
$F_{\lim\_sup}^{Aster}$ (N.mm^{-1})	72,08	100,80	123,41	141,17	156,75
$F_{\lim\_inf}^{Aster}$ (N.mm^{-1})	59,41	84,49	100,61	115,92	129,42

Table 6 : Plate in tension with a centered crack : limit loads results.

LA4 : Axisymmetric tube with a circumferential crack under tension and pressure

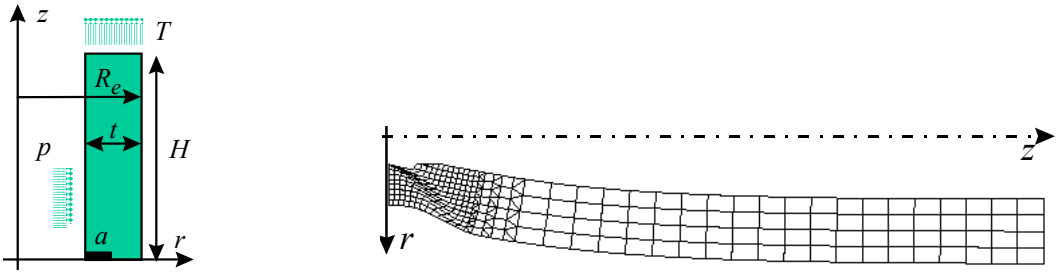

Figure 4: 2D-axis tube with a circumferential crack ; deformed mesh (right) 4300 nodes, 1800 Q8, T6 elements.

material	homogeneous
constitutive relation	perfect plasticity, $\sigma_y = 100 MPa$
geometry	crack : a/t=0.25 ; R_m/t=10.5, H/R_m =0.90 ($R_m = 420mm$).
loading direction	tensile stress T, pressure P (increasing together or only one increasing, the other remaining constant).

Table 7 : Axisymmetric tube with a circumferential crack under tension and pressure : data.

The algorithm provided results with a very satisfactory behaviour. Our results ((F,P) points) with *Code_Aster* are summarised on the figure 5 (with a comparison with analytical simplified lower bound values, taking an admissible stress field defined by two strips, and previous incremental elastic-plastic calculations). The reached value of the regularisation parameter n is 30, for a number of equivalent elastic calculation between 11 and 44. Our results are close to those obtained by other methods participating to the benchmark.

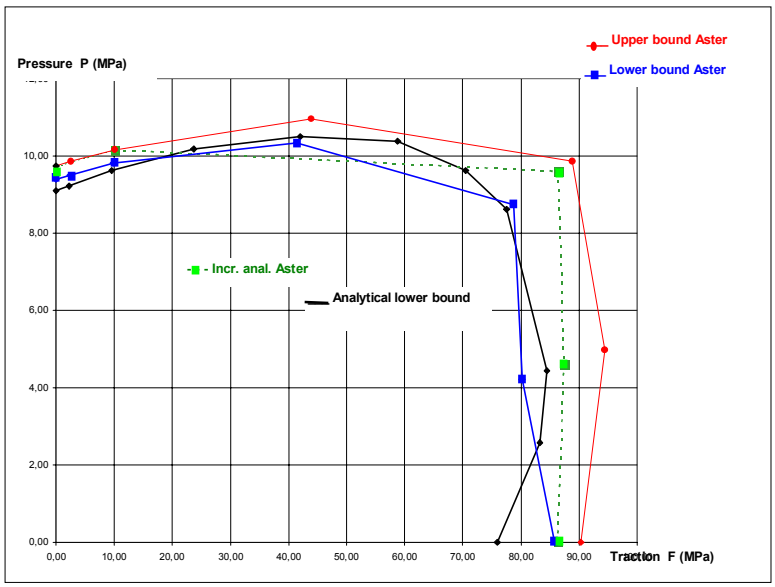

Figure 5: Axisymmetric tube with a circumferential crack ; limit loading boundary.

LA5 : Axisymmetric tube with a semi-elliptical flaw under pressure

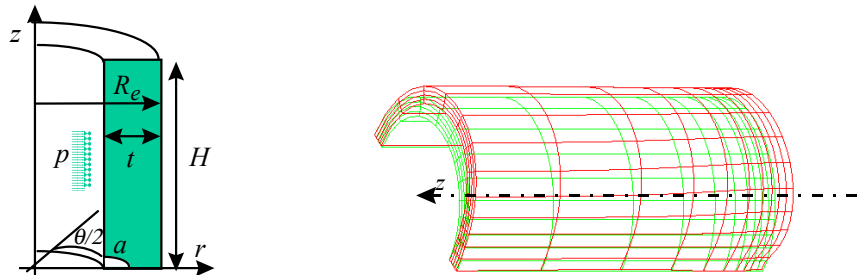

Figure 6: Axisymmetric tube with a semi-elliptical flaw ; deformed mesh (right) : HE20 elements, 3000 nodes.

This case concerns a tube (R_m/t=5, 10, 20) with a flaw : a/t=0.333, $b/\sqrt{R_m t}=0.5$, $\theta=\pi/4;2\pi$, constituted by a homogeneous material ($\sigma_y=100\,MPa$), under pressure with closed end condition. As for the case LA4, the algorithm behaves quite well : we need about 4-5 equivalent elastic calculations in 2D-axis (for $\theta=2\pi$) as well as in 3D, the value of n being equal to 30. Our results from the *Code_Aster* are (in MPa) :

	$P^{lim}_{anal\_inf}$ for $\theta=2\pi$	$P^{-}_{inf\ Code\_Aster}$ ($\theta=2\pi$)	$P^{+}_{sup\ Code\_Aster}$ ($\theta=2\pi$)	$P^{-}_{inf\ Code\_Aster}$ ($\theta=\pi/4$)	$P^{+}_{sup\ Code\_Aster}$ ($\theta=\pi/4$)
$R_m/t=5$	20,99	20,32	21,12	20,54	22,98
$R_m/t=10$	10,51	10,09	10,66		
$R_m/t=20$	5,12	4,85	5,13	5,24	5,75

LA6 : Homogeneous torispherical vessel head under internal pressure

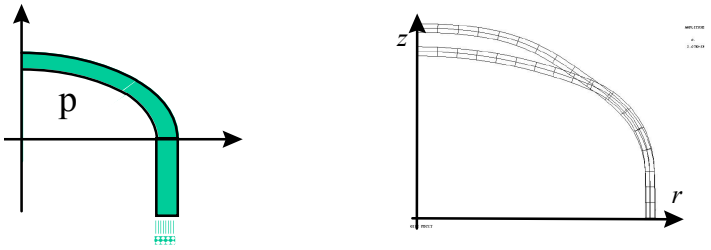

Figure 7: Torispherical vessel head under internal pressure ; deformed mesh (right) : 34 Q8 elements, 141 nodes.

In this case too, the algorithm appears to be very efficient. We can observe on the figure 8 the convergence of the upper an approximated lower bound in terms of the regularisation parameter. For a parameter $n = 71{,}0$, and 19 equivalent elastic calculations, we get the results : $P_{Aster\_\sup}$ =3,9404 MPa, and $P_{Aster\_\inf}$ =3,8372 MPa.

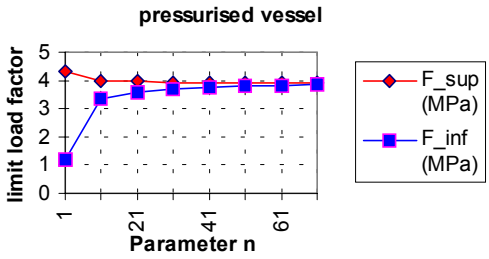

Figure 8: Torispherical vessel head under internal pressure : load factors versus parameter n.

7 COMPARISON WITH AN ELASTOPLASTIC FINITE STRAIN CALCULATION

We considered an elastoplastic pressurised structure with a flaw on the outer wall (see fig.9). With the *Code_Aster* regularised limit analysis algorithm, we get, after 39 equivalent elastic iterations (n=8,25) the following bounding of the limit pressure : 1,353-1,916MPa, for a normalised $\sigma_y = 10{,}0\,MPa$. Moreover, we wanted to assess the predicted collapse mode by a finite strain simulation : indeed, we can suspect that a snap-through can occur, that limit analysis can not idealise. With the *Code_Aster* elastoplastic finite strain incremental simulation (using the Simo-Miehe [xvii] eulerian formulation, which is incrementally objective), assuming isotropic hardening from the experimental strain-stress curve, we get the maximum pressure near from 48,5 MPa, while with limit analysis, we get : 35,1 MPa (if we take the R_e-stress value on the strain-stress curve) or 93 MPa (taking the R_m stress value). The failure modes are quite similar (see fig.9).

We have remarked on this kind of structure (high difference of stiffness between the parts of the structure) that the computing time, for the same mesh are quite similar between limit analysis and elastoplastic finite strain incremental simulation. We can conclude that it can be

safer and not too difficult to use in parallel elastoplastic calculations and limit analysis.

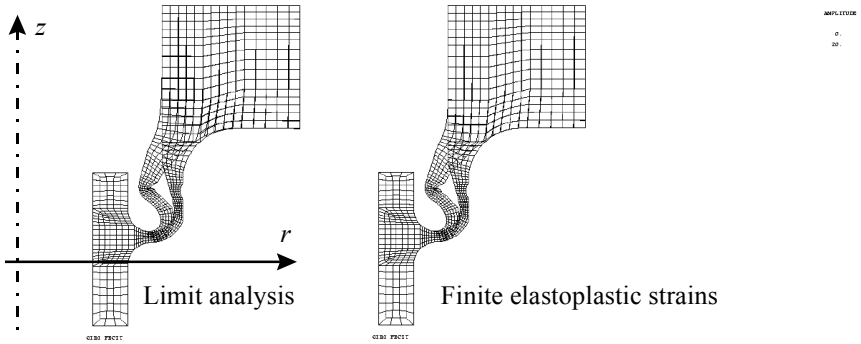

Figure 9: Comparison between the predicted collapses (mesh : 2D-axis, 583 Q8 elements, 1946 nodes).

8 CONCLUSIONS

The limit analysis numerical method presented here has the following characteristics :

- we get an upper bound, with a monotone decreasing with respect to the regularisation parameter, and convergence to the true limit load ;
- the regularised dissipation power involved in the upper bound does not include any elastic term ;
- we get an estimation of the lower bound by post-processing of the obtained numerical stress field, with convergence to the limit load, in the case without dead load. The increasing of the sequence of these lower bounds can not be proved, but is observed on the benchmark tests. This estimation is of practical interest for the applications.

For the 2D-plane strain situation idealisation, we have observed that the main difficulty (of convergence) is not the heterogeneous aspect, but the localisation of the collapse mode (shear bands appear). Adaptive meshing is necessary to provide better results for the bounding. For the 2D-axis and 3D cases, the convergence is good and the calculations are not expensive (especially in 2D-axis) and the results that are been obtained are very close to some available analytical simplified lower bound, and other numerical results. These tests have led to improvements of the method, as well to a better knowledge of its behaviour.

Finally, we can conclude that the proposed numerical method, easy to be implemented into any FEM non linear software, leads to efficient (90% time saved) and sufficient accurate bounding of limit loads with respect to incremental methods or analytical available solutions.

REFERENCES

[i] Hodge P.G., Belytschko T., « Numerical methods for the limit analysis of plates ». *J. Appl. Mech.* 796-802 (1968) ; « Plane stress limit analysis by finite elements ». *A.S.C.E. J. Eng. Mech. Div*., 931-944 (1970).

[ii] Casciaro R., Carlo Di A., Valente G. « Discussion on Plane stress limit analysis by finite

elements by Hodge P.G., Belytschko T ». *A.S.C.E. J. Eng. Mech. Div*., 1560-1566 (1971). Casciaro R., Cascini L. « A mixed formulation and mixed finite elements for limit analysis ». *Int. J. Num. Meth. Eng*., **18**, 211-243, (1982).

[iii] Christiansen E. « Computation of limit loads. » *Int. J. Num. Meth. Eng.,* **17**, 1547-1570 (1981).

[iv] Pastor J., Turgeman S. « Limit Analysis in axisymmetrical problems : numerical determination of complete statical solutions. » *Int. J. Mech. Sci*., **24**, 2, 95-117 (1982).

[v] Heitzer M.. « Traglast- und Einspielanalyse zur Bewertung der Sicherheit passiver Komponenten. » *Thesis*., RWTH Aachen (1999).

[vi] Zouain N., Herskovits J., Borges L., Feijoo R. « An alternative algorithm for limit analysis with nonlinear yield functions. » *Int. J. Solids. Struct*., **30**, 10, 1397-1417 (1993).

[vii] Maghous S. « Détermination du critère de résistance macroscopique d'un matériau hétérogène à structure périodique ». *Thesis* E.N.P.C. Paris, (1991).

[viii] Pastor J., Turgeman S. « Limit Analysis : a linear formulation of the kinematic approach for axisymmetric mechanical problems ». *Int. J. Num. Anal. Meth. Geomech*., **6**, 109-128 (1982).

[ix] Clément D. « Résolution numérique d'un problème modèle en plasticité ». *Thesis*, Univ. Paris Sud (1982).

[x] Gaudrat V. « A Newton type algorithm for plastic limit analysis ». *Comp. Meth. Appl. Mech. Eng.* **88**, 207-224, (1991).

[xi] Yan A.M.. « Contributions to the direct limit state analysis of plastified and cracked structures ». *Thesis*, Univ. Liège, (1999).

[xii] Mercier B. « Sur la théorie et l'analyse numérique de problèmes de plasticité ». *Thesis*, Paris VI, (1977).

[xiii] Friaâ A., Loi de Norton-Hoff généralisée en plasticité et viscoplasticité, *Thesis*, Univ. Paris (1979). Frémond M., Friaâ A. « Les méthodes statique et cinématique en calcul à la rupture et en analyse limite ». *J. Méca. Théo. Appl*., **1**, 6, 881-905 (1982).

[xiv] Guennouni T., Le Tallec P. « Calcul à la rupture : régularisation de Norton-Hoff et lagrangien augmenté ». *J. Méca. Théo. Appl. Mech*., **2**, 1, 75-99, (1982).

[xv] Berak E.G., Gerdeen J.C. « A finite element technique for limit analysis of structures. » *J. Pressure Vessel Technology*, **112**, 138-144 (1990).

[xvi] Joch J., Ainsworth R.A. and Hyde T.H., « Limit load and J-estimates for idealised problems of deeply-cracked welded joints in plane-strain bending and tension ». *Fatigue Fract. Engng. Mater. Struct*., **16**, 10, 1061-1079 (1993).

[xvii] Simo J.C., Miehe C. , « Associative coupled thermoplasticity at finite strains : Formulation, numerical analysis and implementation », *Comp. Meth. Appl. Mech. Eng*., **98**, 41-104, North Holland, (1992).